

## Uniform patterned growth of carbon nanotubes without surface carbon

K. B. K. Teo,<sup>a)</sup> M. Chhowalla, G. A. J. Amaratunga, and W. I. Milne  
*Engineering Department, University of Cambridge, Trumpington Street, Cambridge CB2 1PZ,  
United Kingdom*

D. G. Hasko  
*Microelectronics Research Centre, Cavendish Laboratory, Madingley Road, Cambridge CB3 0HE,  
United Kingdom*

G. Pirio, P. Legagneux, F. Wyczisk, and D. Pribat  
*Thales Laboratoire Central de Recherches, Domaine de Corbeville, 91404 Orsay Cedex, France*

(Received 16 April 2001; accepted for publication 6 July 2001)

In order to utilize the unique properties of carbon nanotubes in microelectronic devices, it is necessary to develop a technology which enables high yield, uniform, and preferential growth of perfectly aligned nanotubes. We demonstrate such a technology by using plasma-enhanced chemical-vapor deposition (PECVD) of carbon nanotubes. By patterning the nickel catalyst, we have deposited uniform arrays of nanotubes and single free-standing aligned nanotubes at precise locations. In the PECVD process, however, detrimental amorphous carbon (*a*-C) is also deposited over regions of the substrate surface where the catalyst is absent. Here, we show, using depth-resolved Auger electron spectroscopy, that by employing a suitable deposition (acetylene, C<sub>2</sub>H<sub>2</sub>) to etching (ammonia, NH<sub>3</sub>) gas ratio, it is possible to obtain nanotube growth without the presence of *a*-C on the substrate surface. © 2001 American Institute of Physics.

[DOI: 10.1063/1.1400085]

The remarkable structural, electrical, and mechanical properties of carbon nanotubes have generated considerable interest in their application in a myriad of nanoelectronic devices,<sup>1</sup> scanning probes,<sup>2</sup> field-emission sources,<sup>3</sup> and supercapacitors.<sup>4</sup> High-quality single and multiwalled carbon nanotubes can be deposited using high-pressure arcs,<sup>5</sup> laser ablation,<sup>6</sup> and chemical-vapor deposition (CVD).<sup>7</sup> The advantage of CVD synthesis is that it is a controllable and deterministic<sup>8</sup> catalytic growth process—that is, the growth location of the nanotube is precisely determined by the location of the catalyst on the substrate. This enabling technology allows us to construct useful nanotube devices by using readily available patterning techniques such as lithography to accurately place the catalyst followed by *in situ* nanotube growth.

Patterned arrays of nonaligned and vertically aligned nanotubes have been deposited using various types of CVD.<sup>9–11</sup> Single nanotubes, nucleated using submicron patterned catalysts, can be deposited using plasma-enhanced chemical-vapor deposition (PECVD).<sup>8,12</sup> A major concern of the PECVD growth process, however, is the formation of surface amorphous carbon (*a*-C), which has been largely ignored in the literature. This can cause problems in device fabrication and operation.

In this letter, we show that it is possible to grow uniform arrays of vertically aligned nanotubes at precise locations on Si substrates via lithographic patterning without the deposition of *a*-C. The *a*-C can be almost entirely eliminated from the unpatterned regions by utilizing the appropriate ratio of the deposition gas (i.e., acetylene C<sub>2</sub>H<sub>2</sub>) to the etching gas (ammonia NH<sub>3</sub>). The absence of *a*-C in the unpatterned re-

gions was verified for a C<sub>2</sub>H<sub>2</sub>:NH<sub>3</sub> ratio of 1:5 (20%) using depth-resolved Auger electron spectroscopy.

Nickel catalyst and diffusion barrier thin films were deposited onto doped Si substrates and patterned lithographically using a lift-off process. Both optical lithography and electron-beam lithography (for submicron features) were used to define the Ni catalyst areas. The diffusion barrier layer prevents the formation of NiSi<sub>x</sub> via diffusion above 300 °C and maintains “active” Ni particles for the catalytic nucleation and growth of the nanotubes, resulting in 100% yield of nanotubes. Typical diffusion barrier materials for nanotube growth are SiO<sub>2</sub> and TiN.<sup>13</sup> Upon annealing to the growth temperature of 700 °C, the nickel thin film was found to break up into nanoparticles which seed the growth of the nanotubes. In general, we have found that the thickness of the initial nickel thin film determines the size and density of the nanoparticles formed after annealing, and hence, also controls the diameter, height, and density of the nanotubes.<sup>11,14</sup> After reaching a temperature of 700 °C, the nanotube growth was initiated immediately by introducing NH<sub>3</sub> and C<sub>2</sub>H<sub>2</sub> into the chamber and initiating the direct current (dc) glow discharge. The nanotubes were grown in a bell jar vacuum chamber pumped to a base pressure of 10<sup>-2</sup> Torr using a rotary pump. The glow discharge plasma was initiated using a 1 kW dc generator between the heated substrate holder and a 2 mm Cu anode situated 2 cm from the cathode. All the depositions were carried out at a bias voltage of -600 V, drawing a bias current of 0.1 A. The C<sub>2</sub>H<sub>2</sub>:NH<sub>3</sub> ratio was varied from 15% to 75% in order to investigate the influence of the gas composition on the formation of *a*-C. Additional experimental details and growth characteristics using our method are presented elsewhere.<sup>14</sup> Despite being

<sup>a)</sup>Electronic mail: kbkt2@eng.cam.ac.uk

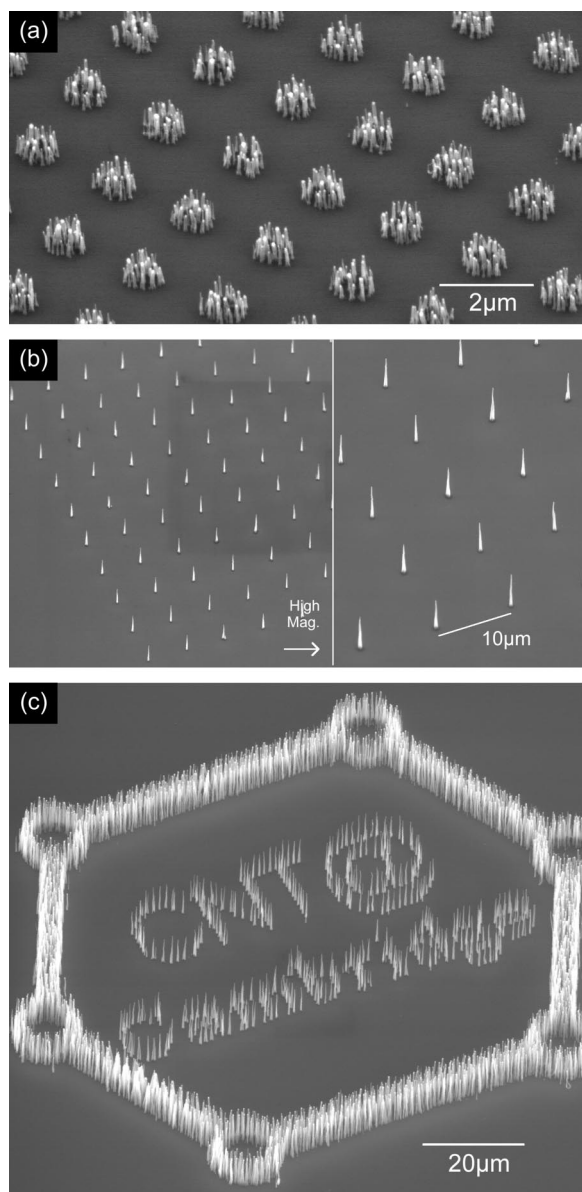


FIG. 1. (a) Bunches of nanotubes ( $\sim 100$  nm in diameter) are deposited on  $1 \mu\text{m}$  nickel dots because the nickel catalyst film breaks up into multiple nanoparticles. (b) Single nanotubes are deposited when the nickel dot size is reduced to  $100$  nm as only a single nickel nanoparticle is formed from the dot. (c) Demonstration of high yield, uniform, and selective growth of nanotubes at different densities.

perfectly aligned, the nanotubes contain structural defects and are sometimes referred to in the literature as nanofibers.

Figure 1 shows various examples of nanotube arrays deposited using this process. Figure 1(a) shows nanotubes grown from  $1 \mu\text{m}$  Ni dots. It can be seen that several nanotubes with diameters  $\sim 100$  nm are nucleated on each dot. Thus, when the patterned Ni dot size is decreased to  $\sim 100$  nm, single nanotubes on each Ni dot can be grown, as shown in Fig. 1(b). Since the size of the patterned Ni islands is uniform, the corresponding nanotubes are also uniform in height and diameter. The nanotubes are tapered in shape due to the plasma etching effect of  $\text{NH}_3$ . The spacing between the nanotubes can be controlled via lithography while the height of the nanotubes is controlled by the deposition time.<sup>14</sup> The nanotube array of Fig. 1(b) satisfies the prerequisite of intertube distance ( $10 \mu\text{m}$ ) being twice that of the

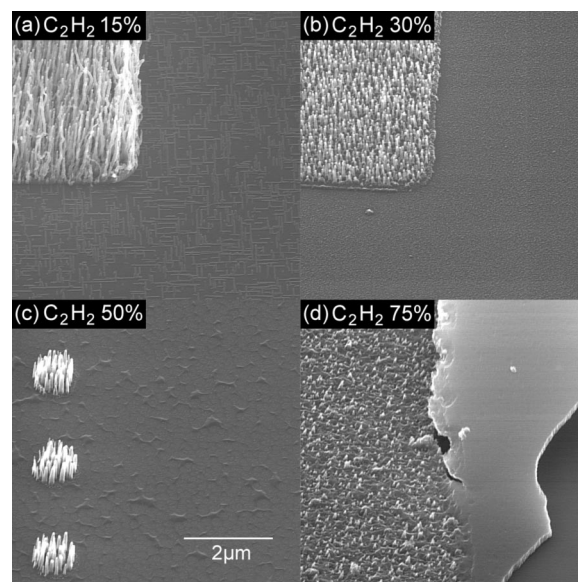


FIG. 2. Scanning electron microscope images of patterned substrates deposited at different  $\text{C}_2\text{H}_2$  to  $\text{NH}_3$  ratios. The morphology of the unpatterned Si area clearly changes from being etched at a low  $\text{C}_2\text{H}_2$  ratio to being covered by a thick, delaminating  $a\text{-C}$  film for high  $\text{C}_2\text{H}_2$  ratios. Note that at the  $\text{C}_2\text{H}_2$  ratio of 75%, nanotube tip heads can be observed to protrude from the  $a\text{-C}$  film on the patterned area.

nanotube height ( $5 \mu\text{m}$ ) to reduce the electric-field shielding from adjacent tubes for field-emission applications.<sup>10</sup> The ability to control the density of the nanotubes is further demonstrated by the lithographic pattern shown in Fig. 1(c).

The tip-growth mechanism (i.e., the Ni nanoparticle is found on top of all our nanotubes) is favored in our process because the nickel nanoparticle is easily detached from the diffusion barrier when growth initiates. We also are able to grow nanotubes which are uniform in height that is determined by the deposition time using the tip-growth mechanism. In contrast, the deposition rate drops off in the base growth of the nanotubes on flat Si substrates due to the catalyst being covered by carbon layers.<sup>11</sup>

Although our PECVD method yields uniform and aligned nanotubes, a potential problem arises from the simultaneous deposition of  $a\text{-C}$ . Unlike nanotubes which exhibit preferential growth at catalyst sites,  $a\text{-C}$  is deposited over the entire substrate. The role of  $\text{NH}_3$  in the plasma is to etch carbon, and thus a balance has to be struck between the growth of nanotubes and removal of  $a\text{-C}$ . Patterned regions with the Ni catalyst and unpatterned areas after nanotube growth at varying  $\text{C}_2\text{H}_2:\text{NH}_3$  ratios are shown in Fig. 2. Note that nanotube growth can only be observed on regions where the Ni catalyst is present. The nanotubes are characteristically different at varying gas ratios, in agreement with our previous results.<sup>14</sup> The unpatterned regions on the substrate are also different depending on the gas ratio used. Anisotropic etching of the Si substrate can be readily seen when the  $\text{C}_2\text{H}_2$  concentration is 15%, indicating that the etching from  $\text{NH}_3$  is greater than the deposition of  $a\text{-C}$ . At higher  $\text{C}_2\text{H}_2$  concentrations, we observe the different morphologies of the  $a\text{-C}$  layer as its thickness increases on the unpatterned areas of the substrate. In fact, at a 75% ratio of  $\text{C}_2\text{H}_2$ , we observe peeling of the  $a\text{-C}$  film on the unpatterned area and tip-shaped nanotube heads<sup>14</sup> protruding from the  $a\text{-C}$  on the

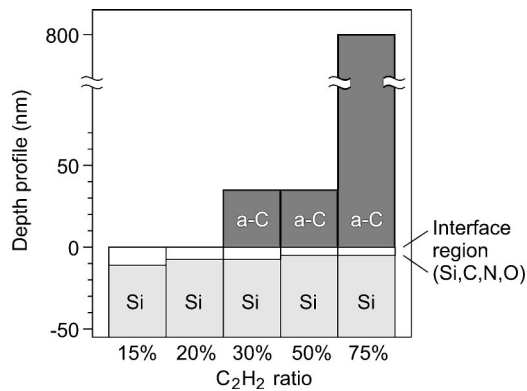


FIG. 3. Summary of depth-resolved Auger chemical analysis on the unpatterned Si areas of samples deposited at different  $C_2H_2$  ratios. Below 30%, no  $a$ -C is detected. In all PECVD cases, a thin interface layer is detected due to the reaction of ionized  $C_2H_2/NH_3$  species in the plasma with the Si surface.

patterned nickel area. Thus, the optimal  $C_2H_2$  ratio for “clean” nanotube deposition lies between 15% and 30%.

The chemical composition of the unpatterned Si areas was investigated by Auger electron spectroscopy (AES) using a Physical Electronic PHI 680 Auger nanoprobe. An *in situ* 2 keV Ar-ion gun was used to sputter the surface and provide depth-resolved chemical analysis. For  $C_2H_2$  ratios of 30% and above,  $a$ -C (with only 5%–10% atomic N) is detected on the surface of the film. By operating at ratios <30%, we can achieve nanotube growth without amorphous-carbon deposits. The thickness of the amorphous carbon increases at ratios >30% because the etching effect of  $NH_3$  becomes less significant. The AES depth profile results are summarized schematically in Fig. 3. In addition to the  $a$ -C layer, an interface layer of 5–10 nm consisting of Si, C, N, and O was detected in the Auger depth profile experiments. The C and N are from the decomposition of  $C_2H_2/NH_3$  and their subsequent reaction/implantation into the Si surface. O is believed to be from the native oxide layer on the Si surface. The interface layer thickness extends deeper into the surface for low  $C_2H_2$  concentrations because of the surface roughness induced by the etching of the Si by  $NH_3$  as observed in Fig. 2(a). The optimal ratio for depositing nanotubes from our apparatus is 20%.

The source of the  $a$ -C on the unpatterned areas is extremely interesting. We have found that the condensation of  $a$ -C only occurs in the presence of a plasma. That is, neither  $a$ -C nor an interface layer was detected on unpatterned regions for thermal deposition of nanotubes in the absence of a plasma using a  $C_2H_2$  ratio of 20% at 700 °C. Thermally deposited “spaghetti-like” nanotubes on a patterned substrate are shown in Fig. 4. This indicates that a plasma is not necessary for the nucleation and growth of nanotubes, but the electric field induced by a plasma is required for the alignment of the tubes.<sup>14</sup> The Si regions outside the Ni catalyst area were found to be pristine with only a thin native oxide layer present, as detected by AES depth analysis. The absence of surface carbon or nitrogen in thermal deposition indicates that condensation of  $a$ -C and the etching of the Si surface are directly related to ionized  $C_2H_2/NH_3$  species in

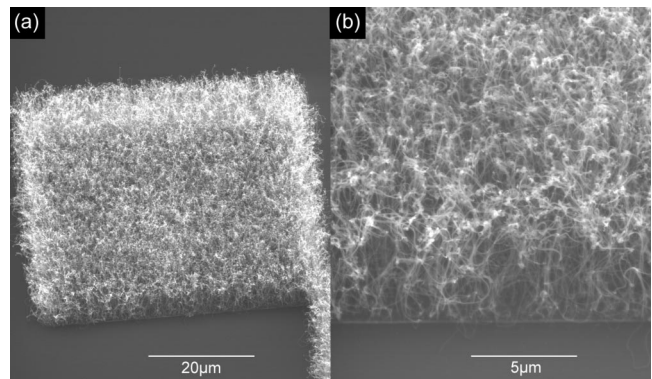


FIG. 4. (a) Patterned spaghetti-like nanotubes [high-magnification image (b)] grown using thermal CVD. No  $a$ -C or interface layer was observed on the unpatterned areas, as confirmed by depth-resolved Auger chemical analysis.

the plasma. For thermal deposition,  $C_2H_2$  is only decomposed by the Ni catalyst for the growth of nanotubes and not over the unpatterned Si surface. Thus, thermal CVD is a clean growth process but at the expense of the nonalignment of the nanotubes.

In conclusion, we have demonstrated the patterned deposition of aligned carbon nanotubes by PECVD. By suitably adjusting the  $C_2H_2$  to  $NH_3$  gas ratios, it is possible to eliminate the undesirable surface carbon on the nonpatterned areas of the substrate. Uniform arrays of single vertically aligned nanotubes have been successfully deposited and the characteristics of these arrays are currently being studied.

This work was funded by the European Commission through the IST-FET project Nanolith and by VA Tech-Reyrolle. One of the authors (K.B.K.T.) acknowledges the support from the Association of Commonwealth Universities and British Council.

- <sup>1</sup>R. Martel, T. Schmidt, H. R. Shea, T. Hertel, and Ph. Avouris, *Appl. Phys. Lett.* **73**, 2447 (1998).
- <sup>2</sup>H. Dai, N. Franklin, and J. Han, *Appl. Phys. Lett.* **73**, 1508 (1998).
- <sup>3</sup>W. A. de Heer, A. Chatelaine, and D. Ugarte, *Science* **270**, 1179 (1995).
- <sup>4</sup>E. Frackowiak, K. Metenier, V. Bertagna, and F. Beguin, *Appl. Phys. Lett.* **77**, 2421 (2000).
- <sup>5</sup>S. Iijima, *Nature (London)* **363**, 603 (1993).
- <sup>6</sup>A. Thess, R. Lee, P. Nikolaev, H. J. Dai, P. Petit, J. Robert, C. H. Xu, Y. H. Lee, S. G. Kim, A. G. Rinzler, D. T. Colbert, G. E. Scuseria, D. Tomaneck, J. E. Fischer, and R. E. Smalley, *Science* **273**, 483 (1996).
- <sup>7</sup>A. M. Cassell, J. A. Raymakers, J. Kong, and H. J. Dai, *J. Phys. Chem. B* **103**, 6484 (1999).
- <sup>8</sup>V. I. Merkulov, D. H. Lowndes, Y. Y. Wei, G. Eres, and E. Voelkl, *Appl. Phys. Lett.* **76**, 3555 (2000).
- <sup>9</sup>Z. F. Ren, Z. P. Huang, J. W. Xu, J. H. Wang, P. Bush, M. P. Siegal, and P. N. Provencio, *Science* **282**, 1105 (1998).
- <sup>10</sup>L. Nilsson, O. Groening, C. Emmenegger, O. Kuettel, E. Schaller, L. Schlapbach, H. Kind, J. M. Bonard, and K. Kern, *Appl. Phys. Lett.* **76**, 2071 (2000).
- <sup>11</sup>C. Bower, O. Zhou, W. Zhu, D. J. Werder, and S. Jin, *Appl. Phys. Lett.* **77**, 2767 (2000).
- <sup>12</sup>Z. F. Ren, Z. P. Huang, D. Z. Wang, J. G. Wen, J. W. Xu, J. H. Wang, L. E. Calvet, J. Chen, J. F. Klemic, and M. A. Reed, *Appl. Phys. Lett.* **75**, 1086 (1999).
- <sup>13</sup>A. M. Rao, D. Jacques, R. C. Haddon, W. Zhu, C. Bower, and S. Jin, *Appl. Phys. Lett.* **76**, 3813 (2000).
- <sup>14</sup>M. Chhowalla, K. B. K. Teo, C. Ducati, N. L. Rupasinghe, G. A. J. Amaratunga, A. C. Ferrari, D. Roy, J. Robertson, and W. I. Milne, *J. Appl. Phys.* (submitted).